






## Wrapped Exponential Distribution Generalizations for Circular Data Analysis

E. Zinhom<sup>1,\*</sup> , M. M. Nassar<sup>1</sup>, S. S. Radwan<sup>2</sup> , A. Elmasry<sup>1</sup> 

<sup>1</sup> Department of Mathematics, Faculty of Science, Ain Shams University, Cairo, Egypt

<sup>2</sup> Department of Mathematics, Faculty of Science Girls Section, AlAzhar University, Cairo, Egypt

Received: 03/08/2024, Revised: 04/11/2024, Accepted: 21/12/2024, Published online: 24/12/2024

**Abstract:** Circular distributions play a crucial role in modeling data characterized by angular properties, offering indispensable tools for analyzing angles, phases, or periodic events. The versatility of these distributions is evident in their application across various domains. There are various strategies available for constructing circular distributions. Exponential distribution is one of the most important models for analyzing lifetime data. In this work, we discuss the wrapped exponential distribution and its properties. Furthermore, we propose three extensions to the wrapped exponential distribution based on the Marshall-Olkin, type I half logistic, and exponentiated generalized generators. We present several mathematical characteristics of these extensions and a unique linear representation of their densities. We investigate the maximum likelihood, least squares, and weighted least squares estimators of the unknown parameters and conduct a simulation study to evaluate their performance. Finally, we compare our novel models against the wrapped exponential and transmuted wrapped exponential distribution using real data in four applications.

**Keywords:** circular distributions, wrapped exponential, trigonometric moments, Marshal-Olkin family, exponentiated generalized family.

**2020 AMS Subject Classifications:** 62E15.

### 1. Introduction

Direction measurements play a critical role in various scientific fields. Geologists, for instance, rely on directional measurements to determine the position of the Earth's magnetic pole [1]. Similarly, biologists are interested in the orientation of animals or the flight paths of birds [2, 3]. Image analysis has made it possible to collect multiple direction measurements per sample quickly using computers. However, when dealing with large sample sizes, it is crucial to use circular statistical tests that are appropriate for this scenario [4]. Circular statistical analysis is commonly used in the analysis of phase features from radar imagery [5] and time series analysis of wind speeds and directions [6]. In modern times, extensive

\* Corresponding author e-mail: [esmailzinhom@gmail.com](mailto:esmailzinhom@gmail.com)

databases of DNA and protein sequences are readily available, and structural bioinformatics aims to predict their associated three-dimensional structures. Dihedral angles, assuming ideal bond lengths and angles, are often used mathematically to describe these structures. However, it has been recognized that developing probabilistic models of these angles in proteins can be highly advantageous [7]. Circular data is not limited to compass measurements but can also be obtained from clocks. Whether using a 24-hour clock or a 12-month period, representing time data on a circle is convenient when the endpoints are naturally linked, such as 0.00a.m. and 12.00p.m. or January 1 and December 31. Recently, political scientists [8] have acknowledged the benefits of this approach in gaining information from circular data. To expand the range of applications in this context, researchers have developed circular distributions with various features.

Using established probability distributions on the real line or plane, several techniques can produce a wide range of useful and novel circular models. Below are some of the common techniques:

1. Offset distributions: This technique involves reducing a bivariate linear random variable to only its directional component. These distributions are referred to as offset distributions.
2. Maximal entropy distributions: This method involves describing characteristics like maximal entropy to construct circular models. The von Mises distribution is an example of a maximal entropy distribution.
3. Wrapped distributions: This technique involves wrapping a linear distribution around the unit circle to create a circular distribution. Examples of wrapped distributions include the wrapped normal distribution and the wrapped Cauchy distribution.

For many years, fitting densities to data has been an essential aspect of statistical analysis. Statistical distributions are highly valuable for describing and predicting real-world phenomena, and over the past few decades, numerous

extended distributions have been developed by introducing one or more parameters to a baseline distribution. These distributions have been used to model data across various disciplines, including reliability engineering [9], survival analysis [10], demography [11], and actuarial science [12].

One way to create new, more flexible families of distributions is by adding parameters to an existing distribution. This technique has been widely used in statistical literature to establish various types of distributions. For instance, the Marshal-Olkin-G generator was developed to add a new parameter to baseline distribution [13]. Other examples include the Beta-G [14], the Gamma-G [15], the Kumaraswamy-G [16], the Exponentiated-G [17], and the type-I-half-logistic [18] generators. These generators have been used to create families of distributions that are widely applicable in different fields of study.

The circular Cardioid distribution has been extended in four different ways by Paula et al. [19]. These extensions include beta cardioid, Kumaraswamy cardioid, gamma cardioid, and Marshal-Olkin cardioid distributions.

The exponential distribution is one of the most significant distributions for modeling time-related events and has numerous practical applications. Therefore, the wrapped exponential distribution (WE), which has a probability density function (pdf) and a cumulative distribution function (cdf), has gained considerable attention [20]. The pdf and cdf of WE are given by Equations (1) and (2), respectively:

$$g(\theta | \lambda) = \frac{\lambda e^{-\theta\lambda}}{1 - e^{-2\pi\lambda}}, \quad \theta, \lambda > 0, \quad (1)$$

$$G(\theta | \lambda) = \frac{1 - e^{-\theta\lambda}}{1 - e^{-2\pi\lambda}}, \quad \theta, \lambda > 0. \quad (2)$$

In their study, Yilmaz and Biçer [21] presented an expansion of the WE distribution using the transmutation method and examined its mathematical properties. In this work, we introduce three new expansions of the WE distribution using three well-known generators: Marshal-Olkin-G, type-I-half-logistic-G, and exponentiated generalized-G. These expansions result in pdfs that have a unique linear form obtained by weighting the core term of the WE distribution's pdf. As circular distributions find use in many scientific and applied fields, we also investigate the mathematical properties of the proposed distributions, such as the trigonometric moments. To demonstrate the versatility of our approach, we provide four examples from real-world events.

In this paper, we introduce the Marshal-Olkin wrapped exponential (MOWE), type I half logistic wrapped exponential (HLWE), and exponentiated generalized wrapped exponential (EGWE) distributions, along with their general formulas, in Section 2. The trigonometric moments of the general model are discussed in Section 3. The invariance properties of the three proposed models are studied in Section 4. The maximum likelihood (ML), least squares (LS), and weighted least squares (WLS) estimators of unknown parameters are described in Section 5

and a simulation study is conducted in Section 6. Finally, in Section 7, we provide four real data applications, and the paper concludes with a summary of our findings in Section 8.

## 2. Wrapped Exponential Distribution Generalizations

Let  $f(\theta)$  and  $F(\theta)$  represent the pdf and cdf of a base distribution with  $k$  parameters, respectively. We introduce three generators that can be used to create new distributions with additional parameters.

1. The Marshal-Olkin generator [13] is defined by the following pdf and cdf:

$$g_{MO}(x) = \frac{\alpha f(x)}{(\alpha + (1-\alpha)F(x))^2}, \#(3)$$

and

$$G_{MO}(x) = \frac{F(x)}{\alpha + (1-\alpha)F(x)}, \#(4)$$

respectively, where  $\alpha > 0$  is the additional parameter. Using this generator results in a new  $(k+1)$ -parameter distribution.

2. The type-I-half-logistic generator [18] is defined by the following pdf and cdf:

$$g_{HL}(x) = \frac{2\alpha f(x)(1-F(x))^{\alpha-1}}{(1+\{1-F(x)\}^\alpha)^2}, \#(5)$$

and

$$G_{HL}(x) = \frac{1-\{1-F(x)\}^\alpha}{1+\{1-F(x)\}^\alpha}, \#(6)$$

respectively, where  $\alpha > 0$  is the additional parameter. This generator also results in a new  $(k+1)$ -parameter distribution.

3. The exponentiated generalized generator [17] is defined by the following pdf and cdf:

$$g_{EG}(x) = \alpha\beta f(x)\{1-F(x)\}^{\alpha-1}(1-\{1-F(x)\}^\alpha)^{\beta-1}, \#(7)$$

and

$$G_{EG}(x) = (1-\{1-F(x)\}^\alpha)^\beta, \#(8)$$

respectively, where  $\alpha, \beta > 0$  are the two additional parameters. Using this generator results in a new  $(k+2)$  parameter distribution.

It is important to note that the first two generators provide a new  $(k+1)$ -parameter distribution, while the last generator provides a new  $(k+2)$ -parameter distribution.

### 2.1 Marshal-Olkin Wrapped Exponential (MOWE)

The pdf and cdf of the MOWE distribution can be obtained by substituting Equations (1) and (2) into Equations (3) and (4), respectively. The resulting expressions are given by

$$g_1(\theta | \lambda, \alpha) = \frac{\alpha \lambda e^{-\theta \lambda}}{(1 - e^{-2\pi \lambda}) \left( \frac{(1 - \alpha)(1 - e^{-\theta \lambda})}{1 - e^{-2\pi \lambda}} + \alpha \right)^2} \#(9)$$

$$= w_1(\theta | \lambda, \alpha) e^{-\theta \lambda}, \lambda, \alpha > 0, \#(9)$$

and

$$G_1(\theta | \lambda, \alpha) = \frac{1 - e^{-\theta \lambda}}{(1 - \alpha)(1 - e^{-\theta \lambda}) + \alpha(1 - e^{-2\pi \lambda})}, \#(10)$$

respectively, where  $w_1(\theta | \lambda, \alpha) = \frac{\alpha \lambda}{(1 - e^{-2\pi \lambda}) \left( \frac{(1 - \alpha)(1 - e^{-\theta \lambda})}{1 - e^{-2\pi \lambda}} + \alpha \right)^2}$ .

Figure 1 displays the density function of the MOWE distribution for various values of the parameters.

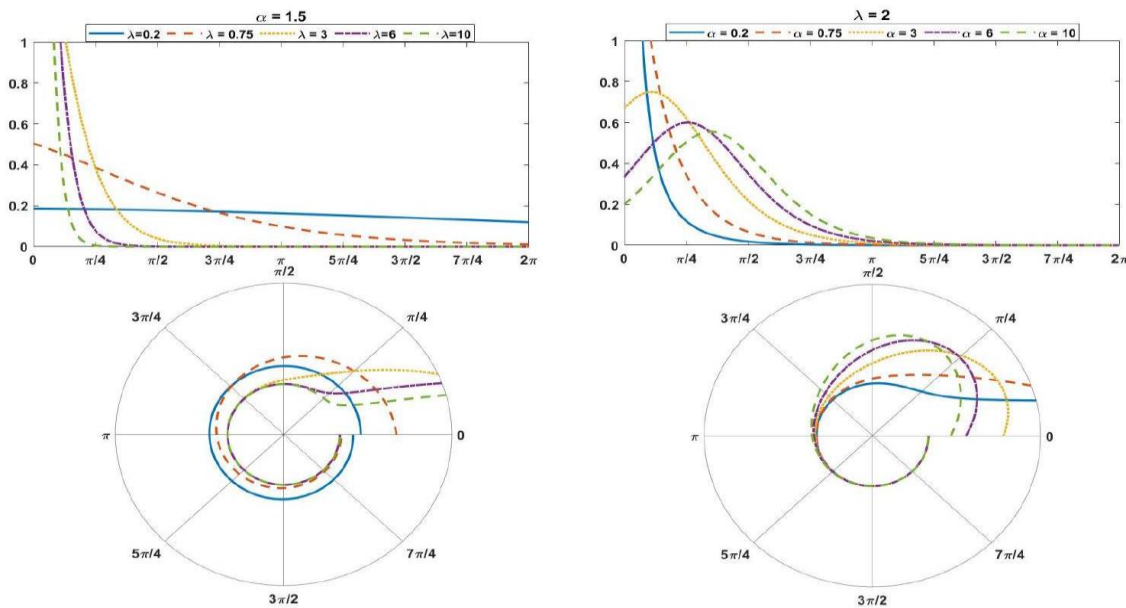


**Figure 1:** Linear and circular representation of MOWE pdf for various values of  $\lambda$  and  $\alpha$ .

### 2.2 Type I Half Logistic Wrapped Exponential (HLWE)

The pdf and cdf of the HLWE distribution can be obtained by applying Equations (1) and (2) to Equations (5) and (6), respectively. The resulting expressions are given by

$$g_2(\theta | \lambda, \alpha) = \frac{2\alpha\lambda e^{-\theta\lambda} \left(1 - \frac{1-e^{-\theta\lambda}}{1-e^{-2\pi\lambda}}\right)^{\alpha-1}}{(1-e^{-2\pi\lambda}) \left\{ \left(1 - \frac{1-e^{-\theta\lambda}}{1-e^{-2\pi\lambda}}\right)^\alpha + 1 \right\}^2} \#$$

$$= w_2(\theta | \lambda, \alpha, \beta) e^{-\theta\lambda}, \lambda, \alpha > 0, \#(11)$$

and

$$G_2(\theta | \lambda, \alpha) = 1 - \frac{2}{1 + \left(\frac{e^{2\pi\lambda}(e^{-\theta\lambda}-1)}{e^{2\pi\lambda}-1} + 1\right)^{-\alpha}}, \#(12)$$

respectively, where  $w_2(\theta | \lambda, \alpha) = \frac{2\alpha\lambda \left(1 - \frac{1-e^{-\theta\lambda}}{1-e^{-2\pi\lambda}}\right)^{\alpha-1}}{(1-e^{-2\pi\lambda}) \left\{ \left(1 - \frac{1-e^{-\theta\lambda}}{1-e^{-2\pi\lambda}}\right)^\alpha + 1 \right\}^2}$ .

Figure 2 displays the density function of the HLWE distribution for various values of the parameters.

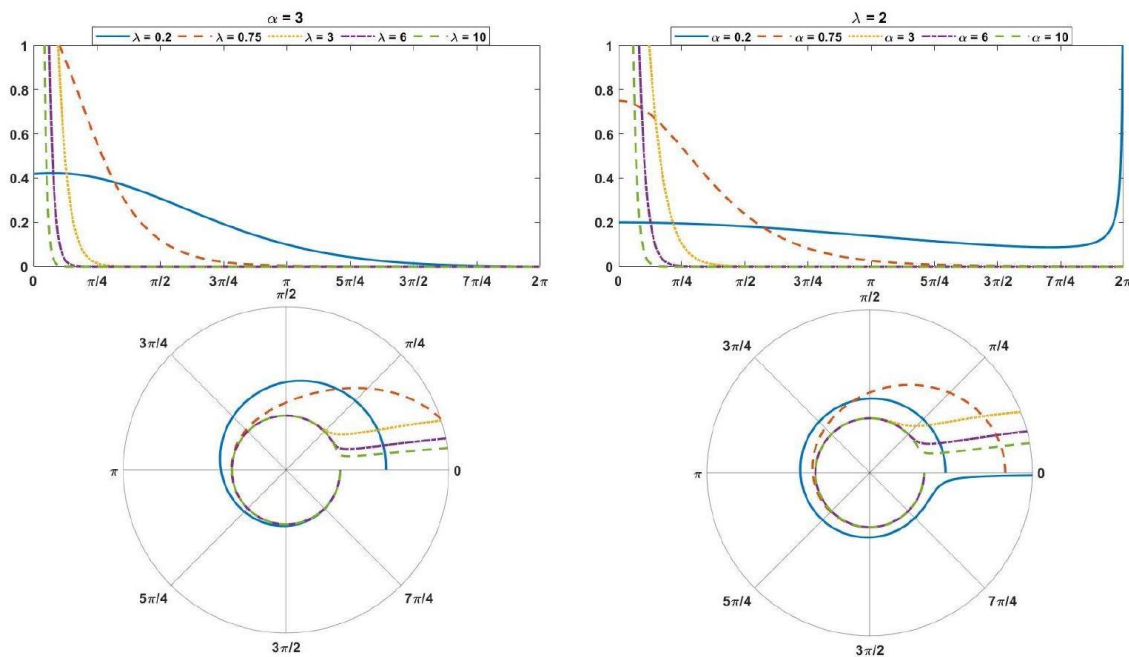


**Figure 2:** Linear and circular representation of HLWE pdf for various values of  $\lambda$  and  $\alpha$ .

### 2.3 Exponentiated Generalized Wrapped Exponential (EGWE)

By substituting Equations (1) and (2) into Equations (7) and (8), respectively, we obtain the pdf and cdf of the EGWE distribution, which are given by

$$g_3(\theta | \lambda, \alpha, \beta) = \frac{\alpha\beta\lambda e^{-\theta\lambda} \left(1 - \frac{1-e^{-\theta\lambda}}{1-e^{-2\pi\lambda}}\right)^{\alpha-1} \left(1 - \left(1 - \frac{1-e^{-\theta\lambda}}{1-e^{-2\pi\lambda}}\right)^\alpha\right)^{\beta-1}}{1 - e^{-2\pi\lambda}}, \#$$

$$= w_3(\theta | \lambda, \alpha, \beta) e^{-\theta\lambda}, \lambda, \alpha, \beta > 0 \#(13)$$

and

$$G_3(\theta | \lambda, \alpha, \beta) = \left( 1 - \left( 1 - \frac{1 - e^{-\theta\lambda}}{1 - e^{-2\pi\lambda}} \right)^\alpha \right)^\beta, \#(14)$$

respectively, where  $w_3(\theta | \lambda, \alpha, \beta) = \frac{\alpha\beta\lambda \left( 1 - \frac{1 - e^{-\theta\lambda}}{1 - e^{-2\pi\lambda}} \right)^{\alpha-1} \left( 1 - \left( 1 - \frac{1 - e^{-\theta\lambda}}{1 - e^{-2\pi\lambda}} \right)^\alpha \right)^{\beta-1}}{1 - e^{-2\pi\lambda}}$ .

Figure 3 displays the density function of the EGWE distribution for various values of the parameters.

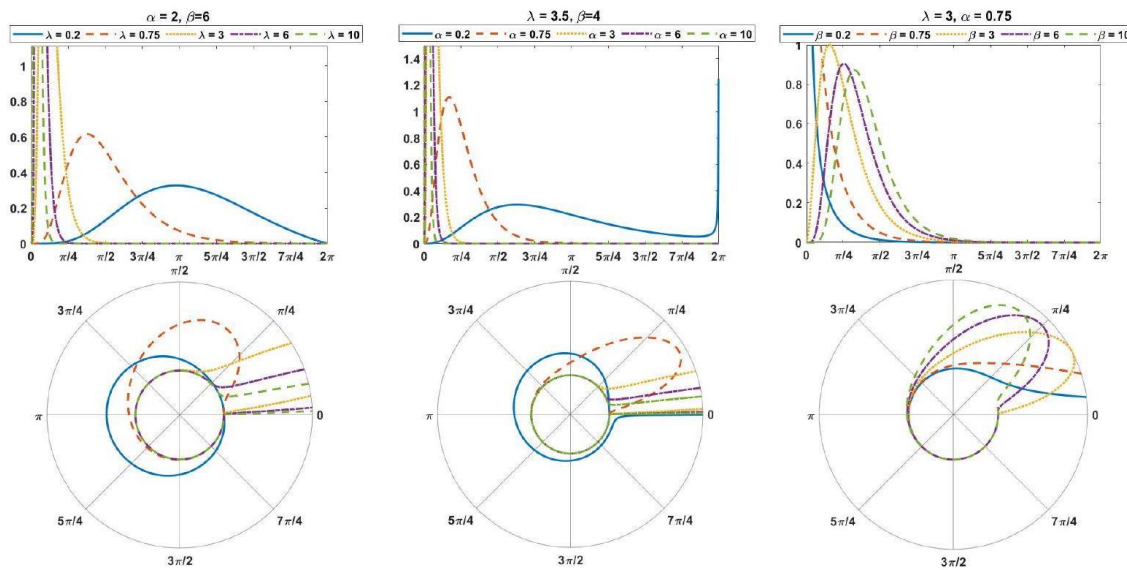


**Figure 3:** Linear and circular representation of EGWE pdf for various values of  $\lambda$ ,  $\alpha$ , and  $\beta$ .

### 2.4 The General Formula for pdfs

The densities of the three extensions, all with the same support, can be expressed in the form

$$g_r(\theta) = w_r(\theta)e^{-\theta\lambda}, r = 1, 2, 3, \#(15)$$

where  $w_r(\theta)$  are the weighted multipliers for the basic pdf kernel  $e^{-\theta\lambda}$ . Thus, the behavior of  $w_r(\theta)$  in (15) is crucial for investigating the properties of the new models.

Figures 4, 5, and 6 depict the three weighted functions  $w_r(\theta)$  for various values of  $\lambda$  and  $\alpha = \beta \in (0,100)$ , with  $\theta \in [0,2\pi)$ .



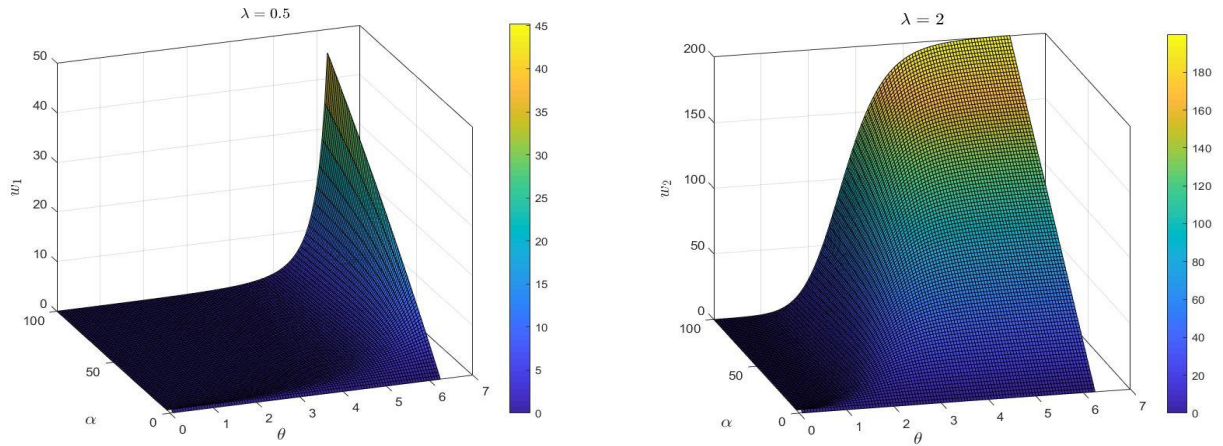


**Figure 4:**  $w_1(\theta | \lambda, \alpha)$  for  $\lambda = 0.5, 2$  and  $\alpha \in (0, 100)$  and  $\theta \in [0, 2\pi)$ .

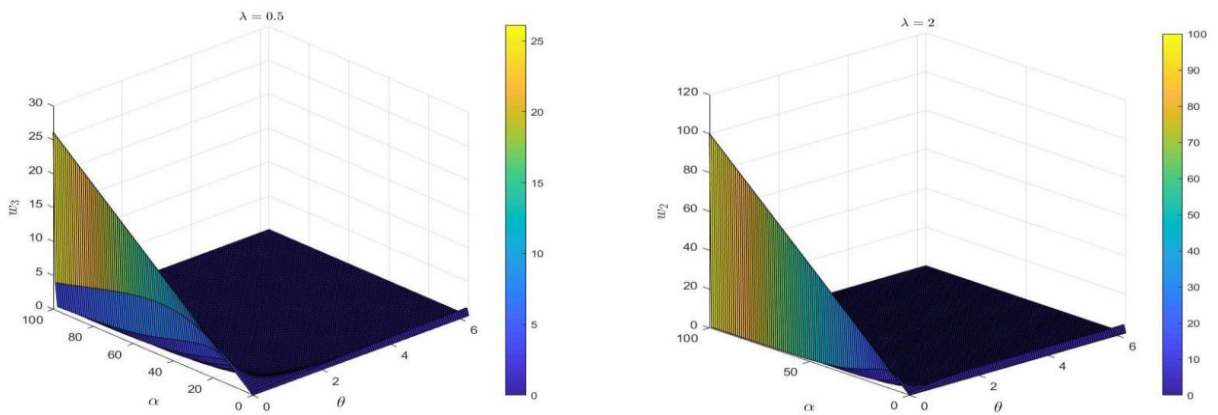


**Figure 5:**  $w_2(\theta | \lambda, \alpha)$  for  $\lambda = 0.5, 2$  and  $\alpha \in (0, 100)$  and  $\theta \in [0, 2\pi)$ .

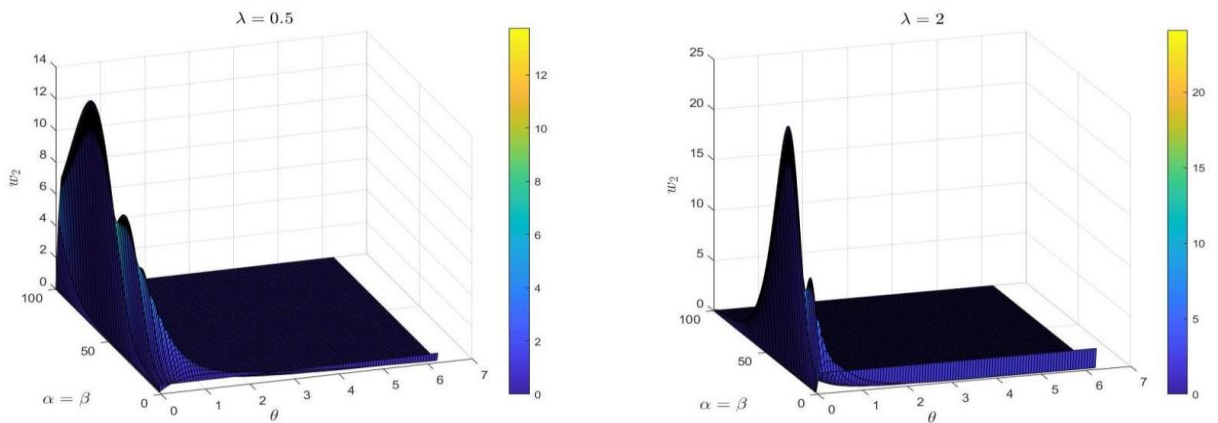


**Figure 6:**  $w_3(\theta | \lambda, \alpha, \beta)$  for  $\lambda = 0.5, 2$  and  $\alpha = \beta \in (0, 100)$  and  $\theta \in [0, 2\pi)$ .

### 3. Trigonometric Moments

In the same way as for distributions over the real line, the characteristic function (CF) can be employed to describe circular distributions. To introduce this concept, we briefly review some fundamental ideas related to circular distributions [22].



Because the circular random variables  $\Theta$  are periodic, the cf can be given by

$$\vartheta_p(\theta) = \vartheta_p = \mathbb{E}(e^{ip\theta}) = \mathbb{E}(e^{ip(\theta+2\pi)}) = e^{2\pi ip} \mathbb{E}(e^{ip\theta}),$$

where  $i = \sqrt{-1}$ , which suggest that  $\vartheta_p = 0$  or  $e^{2\pi ip} = 1$ ; i.e  $p$  has only integer values.

The  $p$  th trigonometric moment of  $\Theta$  is the cf evaluated at an integer  $p$ , and according to Euler's equation, it is determined by

$$\vartheta_p = \mathbb{E}(e^{ip\theta}) = \mathbb{E}(\cos(p\theta) + i\sin(p\theta)) = \mathbb{E}(\cos(p\theta)) + i\mathbb{E}(\sin(p\theta)) = \alpha_p + i\beta_p, \#(16)$$

where  $\alpha_p = \mathbb{E}(\cos(p\theta))$  and  $\beta_p = \mathbb{E}(\sin(p\theta))$ .

$\vartheta_p$  is the mean resultant vector in complex plane with length  $\rho_p = \|\vartheta_p\| = \sqrt{\alpha_p^2 + \beta_p^2} \in [0,1]$  and direction

$$\mu_p = \begin{cases} \tan^{-1}\left(\frac{\beta_p}{\alpha_p}\right), & \text{if } \alpha_p > 0, \beta_p \geq 0, \\ \frac{\pi}{2}, & \text{if } \alpha_p = 0, \beta_p > 0, \\ \tan^{-1}\left(\frac{\beta_p}{\alpha_p}\right) + \pi, & \text{if } \alpha_p < 0, \\ \tan^{-1}\left(\frac{\beta_p}{\alpha_p}\right) + 2\pi, & \text{if } \alpha_p \geq 0, \beta_p < 0, \\ \text{undefined}, & \text{if } \alpha_p = 0, \beta_p = 0. \end{cases}$$

Fundamental measurements of concentration and location are  $\rho_1$  and  $\mu_1$ , respectively. The polar equivalent of  $\vartheta_p$  is

$$\vartheta_p = \rho_p e^{i\mu_p} = \rho_p \cos(\mu_p) + i\rho_p \sin(\mu_p) = \alpha_p + i\beta_p, \#(17)$$

then  $\alpha_p = \rho_p \cos(\mu_p)$  and  $\beta_p = \rho_p \sin(\mu_p)$ .

Our objective is to derive expansions for  $g_i(\theta)$ ,  $i = 1,2,3$ . Starting with our base distribution, we recall that  $g(\theta)$  and  $G(\theta)$  are the pdf and cdf of the wrapped exponential distribution, respectively, given by Equations (1) and (2). The exp-G family with parameter  $k$  has a pdf defined as

$$\begin{aligned} h_k(\theta) &= kg(\theta)G(\theta)^{k-1} \\ &= \frac{k\lambda e^{-\theta\lambda}}{1 - e^{-2\pi\lambda}} \left( \frac{1 - e^{-\theta\lambda}}{1 - e^{-2\pi\lambda}} \right)^{k-1} \\ &= \frac{k\lambda}{(1 - e^{-2\pi\lambda})^k} \sum_{j=0}^{k-1} \binom{k-1}{j} (-1)^j e^{-\theta\lambda(k-j)}. \end{aligned}$$

According to [23], the expansion of MOWE pdf (9) is given by

$$g_1(\theta) = \sum_{k=0}^{\infty} t_k^{(1)} h_{k+1}(\theta),$$

where

$$t_k^{(1)} = \begin{cases} \frac{\alpha(-1)^k}{k+1} \sum_{i=k}^{\infty} \binom{i}{k} (i+1)(1-\alpha)^i, & \text{if } \alpha \in (0,1), \\ \alpha^{-1}(1-\alpha^{-1})^k & \text{if } \alpha > 1. \end{cases}$$

Similarly, as per [17], the expansion of HLWE pdf (11) can be defined as follows:

$$g_2(\theta) = \sum_{k=0}^{\infty} t_k^{(2)} h_{k+1}(\theta),$$

where

$$t_k^{(2)} = \frac{1}{2(2k+1)} \sum_{i=0}^{k-1} \frac{(2i+1)(2k-2i-1)t_i^{(3)}t_{k-i}^{(2)}}{(i+1)(2i+1)}.$$

Furthermore, from [17], we can express the expansion of EGWE pdf (13) as follows:

$$g_3(\theta) = \sum_{k=0}^{\infty} t_k^{(3)} h_{k+1}(\theta),$$

where

$$t_k^{(3)} = \frac{(-1)^k \alpha \beta \Gamma(\beta)}{k!} \sum_{i=0}^{\infty} \frac{(-1)^i \Gamma[(i+1)\alpha]}{(i+1)\Gamma(\beta-i)\Gamma[(i+1)\alpha-k]i!}.$$

Thus, the general expansion of our distributions is expressed as

$$g_r(\theta) = \sum_{k=0}^{\infty} t_k^{(r)} h_{k+1}(\theta), \quad r = 1, 2, 3.$$

Then, the trigonometric moment of the distribution  $g_r$  can be expressed as follows:

$$\begin{aligned} \vartheta_p &= \sum_{k=0}^{\infty} t_k^{(r)} \frac{(k+1)\lambda}{(1-e^{-2\pi\lambda})^{k+1}} \sum_{j=0}^k \binom{k}{j} (-1)^j a^{h_{k+1}} \\ &+ i \sum_{k=0}^{\infty} t_k^{(r)} \frac{(k+1)\lambda}{(1-e^{-2\pi\lambda})^{k+1}} \sum_{j=0}^k \binom{k}{j} (-1)^j b^{h_{k+1}}, \quad r = 1, 2, 3, \end{aligned}$$

where

$$a^{h_{k+1}} = \frac{\lambda(j-k-1)(\cos(2\pi p)e^{2\pi\lambda(j-k-1)} - 1)}{\lambda^2(-j+k+1)^2 + p^2},$$

and

$$b^{h_{k+1}} = \frac{p - e^{2\pi\lambda(j-k-1)}(\lambda(-j+k+1)\sin(2\pi p) + p \cos(2\pi p))}{\lambda^2(-j+k+1)^2 + p^2}.$$

#### 4. Invariance Properties

Circular data has unique characteristics that must be considered in every study, despite having a general structure with the unit circle as support and a closed-form density. There is no stated zero or end for circular data, and natural orientation is arbitrary. The use of well-known circular distributions can lead to incorrect inferences if the difficulties of initial direction and orientation are disregarded, as different experiments can have different starting directions and positive sense of rotation. To avoid making contradictory or incorrect statistical inferences, the distribution used to analyze circular variables must be invariant concerning changes in starting direction (ICID) and orientation changes (ICO). To be ICID and ICO, the characteristic functions of the circular distributions with  $\Theta \in \mathbb{D}$  and  $\Theta^* = \delta(\Theta + \tau)$ , where  $\delta \in \{-1, 1\}$  and  $\tau \in \mathbb{D}$ , must belong to the same functional family with  $\mathbb{D} = [a, b)$  where  $b - a = 2\pi$  and  $\psi$  is a vector of parameters in the pdf  $g_{\Theta}(\cdot; \psi)$  of the circular variable.

$$\vartheta_{\Theta^*}(p) = e^{ip\delta\epsilon}\vartheta_{\Theta}(p\delta).$$

Equations (18) and (3) show that the real and imaginary parts in equations are the same only if  $\delta = 1$  and  $\epsilon = 0$ , meaning that MOWE, HLWE, and EGWE distributions are not ICID and ICO.

If  $g_{\Theta}(\cdot; \psi)$  is not ICO and ICID, the pdf  $g_{\Theta^*}(\cdot; \psi^*)$ , with  $\Theta^* = \delta(\Theta + \tau)$ ,  $\delta \in \{-1, 1\}$ ,  $\tau \in \mathbb{D}$ , and  $\psi^* = (\psi, \delta, \tau) \in \Psi^*$ , is ICO and ICID. Hence, the invariant versions of MOWE, HLWE, and EGWE distributions are given by

$$g_1(\theta^* | \lambda, \alpha, \delta, \epsilon) = \frac{\alpha \lambda e^{-(\delta\theta-\epsilon)\lambda}}{(1 - e^{-2\pi\lambda}) \left( \frac{(1 - \alpha)(1 - e^{-(\delta\theta-\epsilon)\lambda})}{1 - e^{-2\pi\lambda}} + \alpha \right)^2}, \#(19)$$

$$g_2(\theta^* | \lambda, \alpha, \delta, \epsilon) = \frac{2\alpha \lambda e^{-(\delta\theta-\epsilon)\lambda} \left( 1 - \frac{1 - e^{-(\delta\theta-\epsilon)\lambda}}{1 - e^{-2\pi\lambda}} \right)^{\alpha-1}}{(1 - e^{-2\pi\lambda}) \left( \left( 1 - \frac{1 - e^{-(\delta\theta-\epsilon)\lambda}}{1 - e^{-2\pi\lambda}} \right)^\alpha + 1 \right)^2}, \#(20)$$

and

$$g_3(\theta^* | \lambda, \alpha, \beta, \delta, \epsilon) = \frac{\alpha \beta \lambda e^{-(\delta\theta-\epsilon)\lambda} \left( 1 - \frac{1 - e^{-(\delta\theta-\epsilon)\lambda}}{1 - e^{-2\pi\lambda}} \right)^{\alpha-1} \left( 1 - \left( 1 - \frac{1 - e^{-(\delta\theta-\epsilon)\lambda}}{1 - e^{-2\pi\lambda}} \right)^\alpha \right)^{\beta-1}}{1 - e^{-2\pi\lambda}}, \#(21)$$

respectively. These distributions have different formulas and parameters than the original ones and ensure that the characteristic functions of the circular distributions are invariant to changes in starting direction and orientation.

## 5. Estimation

### 5.1 Maximum likelihood method

The maximum likelihood technique is the most often used of the several methods for estimating the parameters that have been put out in the literature. So, a brief overview of the ML estimate of the pdf family's parameters is included in this section.

Let an observed sample  $\theta_1, \theta_2, \dots, \theta_n$  from a random sample has pdf (15). The associated likelihood function can be denoted by

$$\begin{aligned} L(\lambda, \alpha, \beta) &= \prod_{j=1}^n g_r(\theta_j) \\ &= \prod_{j=1}^n w_r(\theta_j) e^{-\lambda \theta_j}, \quad r = 1, 2, 3. \end{aligned}$$

The log-likelihood function is

$$\begin{aligned} l(\lambda, \alpha, \beta) &= \sum_{j=1}^n (\log w_r(\theta_j) - \lambda \theta_j) \\ &= \sum_{j=1}^n \log w_r(\theta_j) - \lambda \sum_{j=1}^n \theta_j, \quad r = 1, 2, 3. \end{aligned}$$

Then

$$\begin{aligned}\tau_{\lambda,r} &= \frac{\partial l(\lambda, \alpha, \beta)}{\partial \lambda} = \sum_{j=1}^n \frac{1}{w_r(\theta_j)} \frac{\partial w_r(\theta_j)}{\partial \lambda} - \sum_{j=1}^n \theta_j \\ \tau_{\alpha,r} &= \frac{\partial l(\lambda, \alpha, \beta)}{\partial \alpha} = \sum_{j=1}^n \frac{1}{w_r(\theta_j)} \frac{\partial w_r(\theta_j)}{\partial \alpha}.\end{aligned}$$

and

$$\tau_{\beta,r} = \frac{\partial l(\lambda, \alpha, \beta)}{\partial \beta} = \sum_{j=1}^n \frac{1}{w_r(\theta_j)} \frac{\partial w_r(\theta_j)}{\partial \beta},$$

where  $r = 1, 2, 3$ . The ML estimator of the parameters  $\lambda$ ,  $\alpha$ , and  $\beta$  is obtained by solving the set of nonlinear equations  $\tau_{\lambda,r} = \tau_{\alpha,r} = \tau_{\beta,r} = 0$

Solving the set of nonlinear equations can be challenging, and various numerical methods can be used to obtain the ML estimator. These methods include the Newton-Raphson method, the Fisher-scoring method, and the Broyde Fletcher-Goldfarb-Shanno (BFGS) method. Ultimately, the ML estimator provides the values of the parameters that maximize the likelihood of observing the given data, given the proposed model.

For the model  $g_r(\theta)$ , the partitioned observed information matrix has the following structure (for  $r = 1, 2$ )

$$\begin{aligned}\mathbb{I}_r(\lambda, \alpha, \beta) &= - \begin{pmatrix} \tau_{\lambda\lambda,r} & \tau_{\lambda\alpha,r} & \tau_{\lambda\beta,r} \\ \tau_{\alpha\lambda,r} & \tau_{\alpha\alpha,r} & \tau_{\alpha\beta,r} \\ \tau_{\beta\lambda,r} & \tau_{\beta\alpha,r} & \tau_{\beta\beta,r} \end{pmatrix} \\ &= - \left\{ \tau_{ab,r} = \frac{\partial^2 l(\lambda, \alpha, \beta)}{\partial a \partial b} \text{ for } a, b = \lambda, \alpha, \beta \right\},\end{aligned}$$

where

$$\tau_{ab,r} = \begin{cases} \sum_{j=1}^n \left( \frac{-1}{w_r(\theta_j)^2} \left( \frac{\partial w_r(\theta_j)}{\partial a} \right)^2 + \frac{1}{w_r(\theta_j)} \frac{\partial^2 w_r(\theta_j)}{\partial^2 a} \right) & \text{if } a = b \\ \sum_{j=1}^n \left( \frac{-1}{w_r(\theta_j)^2} \frac{\partial w_r(\theta_j)}{\partial a} \frac{\partial w_r(\theta_j)}{\partial b} + \frac{1}{w_r(\theta_j)} \frac{\partial^2 w_r(\theta_j)}{\partial a \partial b} \right) & \text{if } a \neq b. \end{cases}$$

Under the usual regularity criteria, we obtain the Fisher information matrix  $\mathbb{F}_r(V) = E(\mathbb{I}_r(V))$  for interval estimation of the parameters in  $g_r(\theta)$ , where  $V = (\lambda, \alpha, \beta)^T$ . According to [24]  $\sqrt{n}(\hat{V} - V) \xrightarrow{D} N_3(0, \bar{\mathbb{F}}_r(V))$ , where  $\bar{\mathbb{F}}_r = \mathbb{F}_r/n$  is the unit Fisher information matrix, "

$N_k(\mu, \Sigma)$  is  $K$ -dimensional multivariate normal distribution with mean vector  $\mu$  and variance covariance matrix  $\Sigma$ , and " $\xrightarrow{D}$ " means convergence in distribution.

The computation of the Fisher information matrix can be a challenging task, and its complexity often makes it intractable. As a solution, we can use the observed information matrix  $\mathbb{I}_r$  as a substitute for the Fisher information matrix  $\mathbb{F}_r$ .

Although the observed information matrix is an approximation of the Fisher information matrix, it provides a practical and efficient alternative that can be used to estimate the standard errors and confidence intervals of the estimated parameters. This is particularly useful in cases where the computation of the Fisher information matrix is not feasible. The numerical outcomes obtained using the observed information matrix can be reliable and accurate, allowing for valid statistical inference. Therefore, we will use this final method to estimate the standard errors and confidence intervals of the estimated parameters.

## 5.2 Least squares method

The LS method for unknown parameter estimation is a well popular technique, but biased LS estimates are a common problem in statistical inference, particularly when heteroscedasticity is present. Heteroscedasticity refers to a situation where the variance of the error term is not constant across the range of the predictor variable. In such cases, the LS estimates tend to be biased toward the observations with smaller variances, leading to unreliable results.

To address this issue, the weighted least squares (WLS) method is a well-known variation of the LS method. The WLS approach assigns weights to each observation proportional to the inverse of its variance. Thus, observations with smaller variances are given more weight, and those with larger variances are given less weight, resulting in estimates that are less biased than the traditional OLS method when heteroscedasticity is present.

To obtain the LS and WLS estimators of the proposed models, we consider a random sample  $\theta_{(1)}, \theta_{(2)}, \dots, \theta_{(n)}$  with pdf (15), where the  $\theta_{(i)}$  are ordered. Let  $r = 1, 2, 3$ . Define

$$LS_{1,r}(\lambda, \alpha, \beta) = \sum_{i=1}^n \left[ G_r(\theta_{(i)}) - \frac{i}{n+1} \right]^2, \#(22)$$

and

$$LS_{2,r} = \sum_{i=1}^n \frac{(n+1)^2(n+2)}{i(n-i+1)} \left[ G_r(\theta_{(i)}) - \frac{i}{n+1} \right]^2, \#(23)$$

where  $G_r(\cdot)$  is one of the proposed cdfs. The LS and WLS estimators of the parameters  $\lambda$ ,  $\alpha$ , and  $\beta$  can be obtained by minimizing Equations (22) and (23) with respect to the corresponding parameter. This is achieved by finding the values of  $\lambda$ ,  $\alpha$ , and  $\beta$  that minimize the objective function defined by these equations.

In the case of LS estimation, the objective function is the sum of the squared differences between the observed and predicted values of the response variable. In contrast, WLS estimation assigns weights to each observation based on the inverse of its variance, and the objective function is the weighted sum of the squared differences [25].

The process of minimizing the objective function can be carried out using optimization techniques, such as gradient descent or Newton's method. Ultimately, the LS and WLS estimators provide estimates of the parameters that best fit the data according to the chosen objective function.

## 6. Simulation Study

A simulation study was conducted using samples drawn from MOWE, HLWE, and EGWE distributions, with sample sizes of 25, 80, 100, 200, and 500. The simulation was repeated 1000 times to obtain the ML, LS, and WLS estimates for the parameters  $\lambda$ ,  $\alpha$ , and  $\beta$ . The average of these estimates was computed. The standard deviation (SD) and the mean square error (MSE) were also computed for each estimate.

The simulation results for the MOWE, HLWE, and EGWE distributions are presented in Tables 1, 2, and 3, respectively. All the computations in this section were performed using MATLAB R2019a modules.

Tables 1, 2, and 3 show that both the SD and MSE decrease as the sample size increases for all parameters settings. This indicates that the estimators are accurate, precise, consistent, and unbiased. It is expected that the ML estimators, being asymptotically unbiased, would exhibit this behavior. Furthermore, the simulation results suggest that the LS and WLS estimators also possess these desirable characteristics. However, the simulation results indicate that the ML estimator perform better than the LS and WLS estimators, as they have lower MSE values.



**Table 1:** The simulation results for MOWE distribution for various values of  $\lambda$  and  $\alpha$ .

Method	n	$\lambda=0.5$			$\alpha=0.75$			$\lambda=0.5$			$\alpha=1$		
		$\hat{\lambda}$	SD	MSE	$\hat{\alpha}$	SD	MSE	$\hat{\lambda}$	SD	MSE	$\hat{\alpha}$	SD	MSE
ML	25	0.779	0.716	0.590	0.892	0.559	0.333	0.786	0.691	0.560	1.226	0.689	0.526
	80	0.495	0.261	0.068	0.845	0.480	0.239	0.497	0.243	0.059	1.132	0.635	0.421
	100	0.494	0.231	0.053	0.832	0.446	0.205	0.496	0.211	0.044	1.103	0.547	0.310
	200	0.492	0.164	0.026	0.778	0.283	0.081	0.498	0.159	0.025	1.064	0.396	0.161
	500	0.500	0.103	0.010	0.769	0.183	0.034	0.498	0.093	0.008	1.018	0.237	0.056
WLS	25	0.670	0.900	0.838	0.731	0.665	0.443	0.668	0.837	0.728	0.998	0.834	0.695
	80	0.466	0.277	0.078	0.807	0.498	0.251	0.473	0.252	0.064	1.082	0.646	0.424
	100	0.469	0.245	0.061	0.799	0.452	0.207	0.472	0.224	0.051	1.057	0.555	0.311
	200	0.484	0.177	0.031	0.770	0.303	0.092	0.486	0.168	0.028	1.040	0.403	0.164
	500	0.496	0.108	0.011	0.764	0.190	0.036	0.493	0.097	0.009	1.008	0.244	0.059
LS	25	0.659	1.018	1.061	0.695	0.694	0.484	0.660	0.853	0.752	0.966	0.895	0.802
	80	0.448	0.297	0.091	0.790	0.531	0.284	0.460	0.264	0.071	1.062	0.671	0.454
	100	0.448	0.267	0.07	0.776	0.480	0.231	0.454	0.243	0.061	1.030	0.579	0.336
	200	0.473	0.197	0.039	0.758	0.325	0.106	0.473	0.184	0.034	1.020	0.426	0.182
	500	0.491	0.121	0.014	0.758	0.205	0.042	0.488	0.107	0.011	1.000	0.259	0.067
Method	n	$\lambda=1$			$\alpha=0.5$			$\lambda=1$			$\alpha=1$		
		$\hat{\lambda}$	SD	MSE	$\hat{\alpha}$	SD	MSE	$\hat{\lambda}$	SD	MSE	$\hat{\alpha}$	SD	MSE
ML	25	1.589	1.609	2.935	0.539	0.383	0.148	1.153	0.527	0.301	1.538	1.364	2.151
	80	1.067	0.341	0.120	0.577	0.264	0.075	1.051	0.262	0.071	1.149	0.495	0.268
	100	1.050	0.304	0.095	0.558	0.224	0.053	1.024	0.238	0.057	1.088	0.425	0.188
	200	1.025	0.202	0.041	0.526	0.147	0.022	1.014	0.159	0.025	1.044	0.269	0.074
	500	1.007	0.126	0.016	0.509	0.093	0.008	1.007	0.098	0.009	1.022	0.169	0.029
WLS	25	1.298	1.382	1.997	0.442	0.381	0.148	1.007	0.0648	0.420	1.403	1.972	4.048
	80	1.008	0.410	0.168	0.547	0.305	0.095	1.019	0.299	0.090	1.113	0.537	0.301
	100	1.021	0.363	0.132	0.545	0.257	0.068	0.993	0.265	0.070	1.053	0.463	0.217
	200	1.012	0.240	0.058	0.521	0.174	0.030	1.002	0.176	0.031	1.029	0.293	0.086
	500	1.003	0.140	0.019	0.507	0.100	0.010	1.004	0.107	0.011	1.018	0.182	0.033
LS	25	1.263	1.407	2.047	0.424	0.392	0.159	0.971	0.689	0.475	1.394	2.124	4.666
	80	0.967	0.480	0.231	0.531	0.334	0.112	0.995	0.343	0.118	1.093	0.586	0.352
	100	0.990	0.436	0.190	0.535	0.294	0.087	0.968	0.301	0.092	1.028	0.499	0.250
	200	0.996	0.290	0.084	0.515	0.199	0.039	0.988	0.200	0.040	1.013	0.319	0.102
	500	0.998	0.168	0.028	0.505	0.115	0.013	0.999	0.125	0.015	1.013	0.202	0.041

**Table 2:** The simulation results for HLWE distribution for various values of  $\lambda$  and  $\alpha$ .

Method	n	$\lambda = 0.5$			$\alpha = 0.75$			$\lambda = 0.5$			$\alpha = 1$		
		$\hat{\lambda}$	SD	MSE	$\hat{\alpha}$	SD	MSE	$\hat{\lambda}$	SD	MSE	$\hat{\alpha}$	SD	MSE
ML	25	0.528	0.054	0.004	0.781	0.071	0.006	0.533	0.060	0.005	1.034	0.091	0.009
	80	0.488	0.222	0.049	0.814	0.243	0.063	0.494	0.247	0.061	1.104	0.363	0.142
	100	0.486	0.205	0.042	0.811	0.220	0.052	0.494	0.247	0.061	1.104	0.363	0.142
	200	0.497	0.138	0.019	0.772	0.136	0.019	0.489	0.166	0.028	1.061	0.246	0.064
	500	0.498	0.090	0.008	0.761	0.088	0.008	0.500	0.104	0.011	1.020	0.148	0.022
WLS	25	0.547	0.357	0.130	1.112	1.065	1.264	0.601	0.587	0.355	1.990	1.851	4.402
	80	0.553	0.304	0.095	0.783	0.321	0.104	0.591	0.393	0.162	1.063	0.530	0.284
	100	0.538	0.276	0.078	0.786	0.277	0.078	0.591	0.393	0.162	1.063	0.530	0.284
	200	0.514	0.174	0.030	0.765	0.168	0.028	0.530	0.245	0.061	1.048	0.362	0.133
	500	0.503	0.110	0.012	0.760	0.108	0.012	0.517	0.143	0.021	1.011	0.201	0.040
LS	25	0.562	0.437	0.195	1.247	1.265	1.847	0.663	0.743	0.579	2.145	1.956	5.132
	80	0.614	0.408	0.180	0.769	0.373	0.139	0.710	0.607	0.413	1.046	0.634	0.404
	100	0.590	0.361	0.138	0.770	0.323	0.105	0.710	0.607	0.413	1.046	0.634	0.404
	200	0.538	0.228	0.053	0.759	0.208	0.043	0.590	0.361	0.138	1.038	0.461	0.214
	500	0.513	0.139	0.019	0.757	0.135	0.018	0.546	0.206	0.044	0.999	0.266	0.071
Method	n	$\lambda = 1$			$\alpha = 0.5$			$\lambda = 1$			$\alpha = 1$		
		$\hat{\lambda}$	SD	MSE	$\hat{\alpha}$	SD	MSE	$\hat{\lambda}$	SD	MSE	$\hat{\alpha}$	SD	MSE
ML	25	1.058	0.113	0.016	0.520	0.051	0.003	1.073	0.125	0.021	1.019	0.073	0.006
	80	0.963	0.425	0.182	0.585	0.229	0.060	0.917	0.458	0.216	1.284	0.469	0.301
	100	0.997	0.387	0.150	0.556	0.196	0.041	0.926	0.468	0.224	1.279	0.471	0.299
	200	1.002	0.284	0.081	0.527	0.125	0.016	0.994	0.474	0.225	1.191	0.449	0.237
	500	0.990	0.165	0.027	0.515	0.076	0.006	1.006	0.402	0.161	1.121	0.373	0.154
WLS	25	0.949	0.716	0.515	1.435	1.798	4.104	1.575	1.717	3.274	2.707	2.369	8.524
	80	1.188	0.771	0.630	0.575	0.359	0.135	1.310	0.748	0.654	1.084	0.616	0.386
	100	1.163	0.658	0.459	0.552	0.315	0.102	1.268	0.730	0.605	1.110	0.613	0.387
	200	1.069	0.434	0.193	0.528	0.189	0.036	1.274	0.681	0.538	1.063	0.568	0.326
	500	1.007	0.231	0.053	0.516	0.107	0.012	1.209	0.622	0.431	1.070	0.520	0.275
LS	25	1.000	0.898	0.806	1.586	1.850	4.596	1.843	2.139	5.281	2.322	1.992	5.712
	80	1.384	1.082	1.318	0.589	0.443	0.204	1.318	0.765	0.685	1.088	0.618	0.390
	100	1.325	0.928	0.965	0.564	0.391	0.157	1.315	0.746	0.656	1.083	0.616	0.386
	200	1.164	0.643	0.440	0.537	0.255	0.067	1.313	0.715	0.608	1.065	0.599	0.363
	500	1.050	0.347	0.123	0.519	0.155	0.024	1.273	0.682	0.539	1.071	0.574	0.334

**Table 3:** The simulation results for EGWE distribution for various values of  $\lambda$ ,  $\alpha$ , and  $\beta$ .

Method	n	$\lambda = 0.5$			$\alpha = 0.5$			$\beta = 0.5$		
		$\hat{\lambda}$	SD	MSE	$\hat{\alpha}$	SD	MSE	$\hat{\beta}$	SD	MSE
ML	25	0.595	0.168	0.037	0.602	0.131	0.027	0.570	0.140	0.025
	80	0.507	0.324	0.105	0.565	0.217	0.051	0.509	0.077	0.006
	100	0.513	0.306	0.094	0.549	0.196	0.041	0.508	0.074	0.006
	200	0.506	0.216	0.047	0.526	0.126	0.017	0.504	0.049	0.002
	500	0.492	0.131	0.017	0.516	0.078	0.006	0.501	0.031	0.001
WLS	25	0.530	0.103	0.012	0.592	0.124	0.024	0.629	0.207	0.059
	80	0.613	0.520	0.283	0.563	0.480	0.234	0.498	0.081	0.007
	100	0.590	0.448	0.209	0.531	0.299	0.090	0.500	0.079	0.006
	200	0.544	0.273	0.076	0.513	0.170	0.029	0.502	0.052	0.003
	500	0.505	0.156	0.024	0.510	0.097	0.010	0.500	0.032	0.001
LS	25	0.533	0.111	0.013	0.596	0.130	0.026	0.632	0.214	0.063
	80	0.684	0.729	0.564	0.618	0.794	0.644	0.491	0.088	0.008
	100	0.634	0.604	0.382	0.570	0.458	0.215	0.494	0.085	0.007
	200	0.590	0.398	0.166	0.518	0.241	0.058	0.500	0.058	0.003
	500	0.518	0.215	0.046	0.514	0.139	0.020	0.499	0.035	0.001
Method	n	$\lambda = 1$			$\alpha = 0.5$			$\beta = 2$		
		$\hat{\lambda}$	SD	MSE	$\hat{\alpha}$	SD	MSE	$\hat{\beta}$	SD	MSE
ML	25	1.917	1.040	1.922	0.584	0.128	0.024	1.535	0.712	0.723
	80	0.991	0.481	0.232	0.584	0.244	0.067	2.032	0.411	0.170
	100	1.000	0.440	0.193	0.558	0.200	0.043	2.028	0.372	0.139
	200	0.986	0.298	0.089	0.536	0.132	0.019	2.011	0.255	0.065
	500	0.991	0.183	0.034	0.514	0.076	0.006	1.998	0.152	0.023
WLS	25	1.367	0.951	1.039	0.526	0.098	0.010	2.090	0.991	0.990
	80	1.198	0.797	0.673	0.558	0.363	0.135	1.977	0.460	0.212
	100	1.134	0.645	0.434	0.539	0.293	0.088	1.967	0.390	0.153
	200	1.043	0.397	0.160	0.526	0.177	0.032	1.986	0.275	0.076
	500	1.009	0.227	0.052	0.510	0.094	0.009	1.990	0.164	0.027
LS	25	1.333	0.855	0.842	0.525	0.098	0.010	2.057	0.933	0.873
	80	1.293	1.030	1.146	0.596	0.484	0.243	1.935	0.510	0.264
	100	1.228	0.878	0.822	0.565	0.401	0.164	1.919	0.424	0.186
	200	1.099	0.564	0.327	0.536	0.239	0.059	1.962	0.308	0.096
	500	1.033	0.330	0.110	0.515	0.135	0.018	1.979	0.194	0.038

## 7. Applications

In this section, we demonstrate the flexibility of our proposed models by presenting four applications. We obtain ML estimates of unknown parameters and calculate the values of several statistical indices, including the Akaike information criterion (AIC), Bayesian information criterion (BIC), Kuiper statistic, and Watson statistic. These statistical measures

provide insight into the goodness-of-fit of our models and allow us to compare their performance across different applications.

We present the results of our first, second, third, and fourth applications in Tables 4, 5, 6, and 7, respectively. These tables are accompanied by Figures 7,8,9, and 10, which display histograms of the data and fitted density plots. The figures provide visual support for the statistical measures presented in the tables and allow for a more intuitive understanding of the goodness-of-fit of our models. The data utilized in this section can be sourced from [26].

### First application

The study aimed to investigate how starhead topminnows orient themselves in both aquatic and terrestrial environments. The researchers dispersed the fish to different beaches in a small forest pond and used a solar compass to track their movements. The fish were able to align their bodies with the position of the sun to move in a specific direction on land. However, on cloudy days, many fish moved randomly as they were unable to maintain the same body position with each leap. The researchers found significant individual differences in terrestrial locomotion. The dataset includes the sun compass directions of 50 Starhead Topminnows under cloudy skies [27].

**Table 4:** Estimated value, AIC, BIC, and Kolmogorov P-Value for the fit based on starhead topminnows data set.

Distribution	$\hat{\lambda}$	$\hat{\alpha}$	$\hat{\beta}$	AIC	BIC	Kuiper	Watson
WE	0.115	-	-	183.642	185.554	0.109	0.034
TWE	0.086	0.093	-	185.871	189.439	0.108	0.033
MOWE	0.000	0.687	-	185.541	189.365	0.1049	0.031
HLWE	0.666	0.623	-	184.415	188.239	0.102	0.023
EGWE	0.402	0.659	1.108	186.033	191.769	0.090	0.018

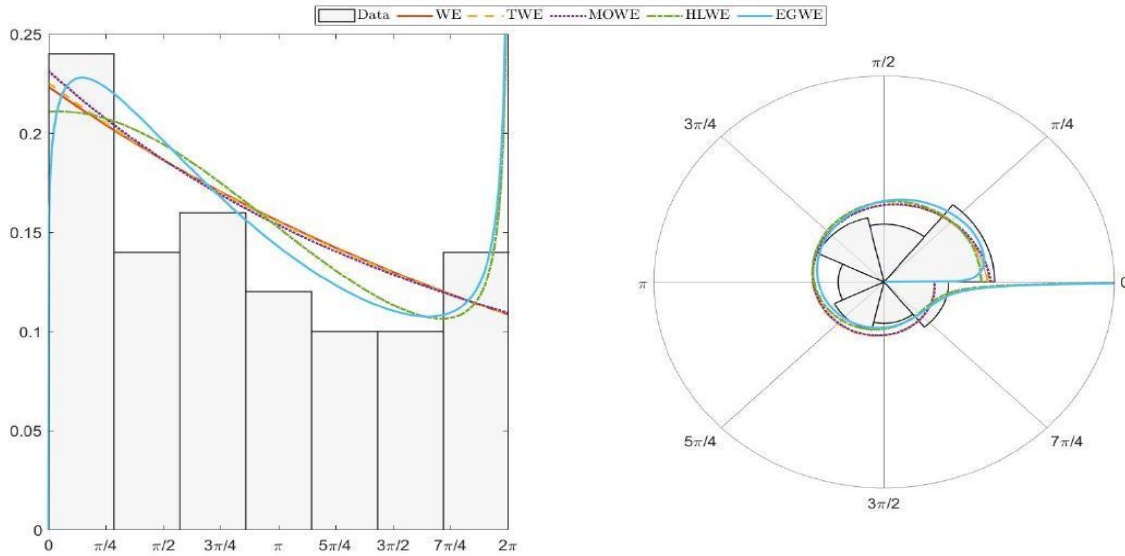


**Figure 7:** Estimated pdfs of the considered distributions for starhead topminnows data set.

The results presented in Table 4 demonstrate that our proposed model provides a better fit to the data compared to the TWE distribution, as indicated by all statistical measures. Furthermore, our model outperforms the WE distribution according to the Kuiper and Watson statistics. These findings suggest that our proposed model is a more appropriate choice for modeling this particular data set compared to the TWE and WE distributions.

**Second application**

The feldspar laths data set provided by [28] consists of measurements of the long-axis orientations of feldspar laths. Feldspar laths are elongated crystals that are commonly found in rocks such as basalt. These measurements are given in degrees and specifically relate to the orientation of feldspar laths in basalt direction. The data set contains a total of 133 measurements, which can be used for further analysis or to study the orientation of feldspar laths in basalt.

**Table 5:** Estimated value, AIC, BIC, and Kolmogorov P-Value for the fit based on feldspar laths data set.

Distribution	$\hat{\lambda}$	$\hat{\alpha}$	$\hat{\beta}$	AIC	BIC	Kuiper	Watson
WE	0.599	-	-	368.873	371.717	1.778	0.750
TWE	0.883	-0.788	-	352.186	357.842	1.840	0.310
MOWE	1.452	6.931	-	337.839	343.495	1.876	0.249
HLWE	$1 \times 10^{-8}$	4.736	-	336.216	341.873	1.856	0.223
EGWE	$5 \times 10^{-8}$	4.040	1.351	347.201	355.638	1.861	0.261

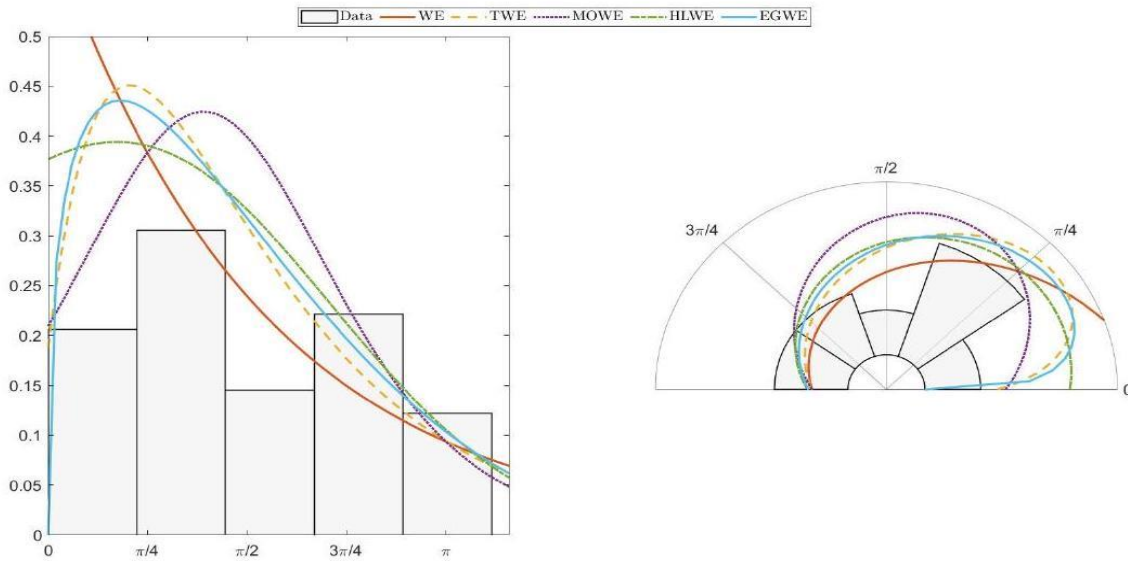


**Figure 8:** Estimated pdfs of the considered distributions for feldspar laths data set.

The results presented in Table 5 indicate that our proposed distribution provides a better fit to the data compared to the WE and TWE distributions, as indicated by all statistical measures except for the Kuiper statistic. The Kuiper statistic suggests that the WE distribution may provide a slightly better fit to the data. However, the overall performance of our proposed distribution across multiple statistical measures suggests that it is still a strong contender for modeling this particular data set.

**Third application**

The turtle data set was provided in [29] and contains information about the orientations of 76 turtles while they lay their eggs. The data set records the direction of the head of each turtle when it begins to dig the egg chamber. The turtle data set is useful for studying the nesting behavior of turtles and can help researchers understand how turtles select nesting sites and the factors that influence their choice of orientation.

**Table 6:** Estimated value, AIC, BIC, and Kolmogorov P-Value for the fit based on turtle data set.

Distribution	$\hat{\lambda}$	$\hat{\alpha}$	$\hat{\beta}$	AIC	BIC	Kuiper	Watson
WE	0.423	-	-	243.349	245.626	0.258	0.337
TWE	0.195	0.626	-	245.444	249.942	0.258	0.336
MOWE	0.628	1.710	-	244.500	248.997	0.239	0.304
HLWE	1.072	0.668	-	243.839	248.337	0.231	0.286
EGWE	1.108	0.637	1.699	240.086	246.745	0.211	0.212

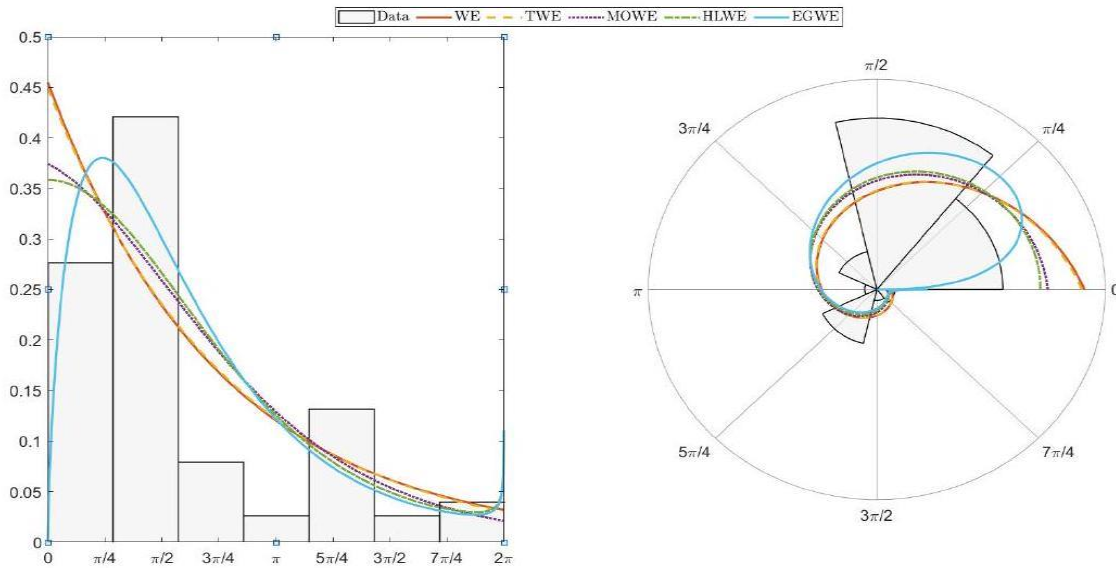


**Figure 9:** Estimated pdfs and cdfs of the considered distributions for turtle data set.

**Fourth application**

The small blue periwinkles, *Nodilittorina unifasciata*, are known for their ability to adapt to changing environmental conditions. In one study, researchers transplanted these periwinkles downshore from their normal habitat to investigate how they would adjust to the change in height.

The researchers found that the periwinkles responded to the change in height by altering both their distance from the water's edge and their orientation with respect to the water's edge. Specifically, the periwinkles moved closer to the water's edge and oriented themselves perpendicular to the shoreline, which allowed them to better withstand the effects of waves and tide. The data set consist of 32 angles of periwinkles orientation [30].

**Table 7:** Estimated value, AIC, BIC, and Kolmogorov P-Value for the fit based on blue periwinkles data set.

Distribution	$\hat{\lambda}$	$\hat{\alpha}$	$\hat{\beta}$	AIC	BIC	Kuiper	Watson
WE	0.530	-	-	96.471	97.803	1.173	0.682
TWE	1.000	-0.900	-	87.360	89.878	1.305	0.433
MOWE	2.253	32.260	-	74.922	77.440	1.522	0.123
HLWE	$3 \times 10^{-7}$	4.587	-	85.942	88.460	1.307	0.401
EGWE	0.328	3.210	4.6567	78.194	81.734	1.511	0.128



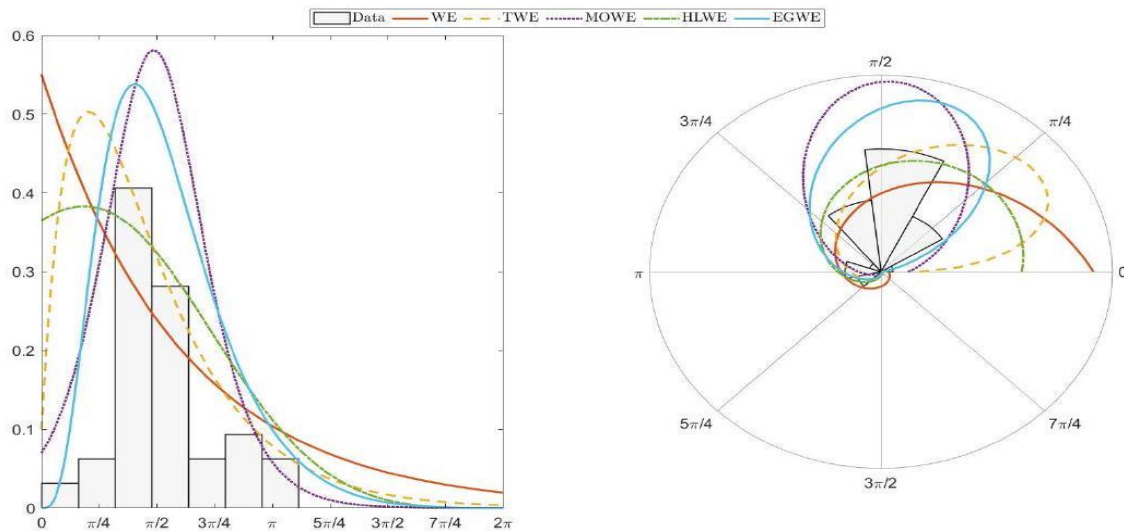


**Figure 10:** Estimated pdfs of the considered distributions for blue periwinkles data set.

In summary of this section, our proposed models were tested across four different applications, and the statistical measures were used to evaluate the goodness-of-fit of our models. In the first and third applications, as shown in Tables 4 and 6, respectively, our proposed models provided a better fit to the data compared to the TWE distribution, as indicated by all statistical measures. Furthermore, our models outperformed the WE distribution according to the Kuiper and Watson statistics.

In the second application, as shown in Table 5, our proposed distributions provided a better fit to the data compared to the WE and TWE distributions, as indicated by all statistical measures except for the Kuiper statistic. The Kuiper statistic suggested that the WE distribution may provide a slightly better fit to the data.

Finally, in the fourth application, as shown in Table 7, our proposed models provided a better fit to the data compared to both the WE and TWE distributions, as indicated by all statistical measures. Overall, these results suggest that our proposed models are generally effective in fitting a range of data sets and outperform commonly used distributions in many cases.

## 8. Conclusion

In our study, we proposed three models of circular distributions. We extended the wrapped exponential distribution by incorporating it into the Marshall-Olkin, type I half logistic, and exponentiated generalized generators while considering a specific adaptation. We derived general formulas for the probability density functions and trigonometric moments of each model to facilitate their use. Additionally, we explained the parameter estimation process

using the maximum likelihood, least squares, and weighted least squares methods. To demonstrate the practicality and adaptability of our proposed models, we applied them to four different real-world examples of circular data sets. We coded the essential calculations and graphics in MATLAB R2019a modules, which we have made available to the readers. Overall, our study provides a practical and useful approach to modeling circular data and offers an alternative to commonly used distributions.

## Statements and Declarations

### Ethical Approval

Ethical approval is not applicable.

### Competing interests

There is no influence by other people or any organization.

### Funding

No funding was received.

### Acknowledgement

We would like to thank the anonymous reviewers for their constructive comments.

## References

- [1] F. Lagona, M. Picone, A. Maruotti, A hidden Markov model for the analysis of cylindrical time series, *Environmetrics*, **26**, 534–544 (2015).
- [2] J. Bulla, F. Lagona, A. Maruotti, M. Picone, A Multivariate Hidden Markov Model for the Identification of Sea Regimes from Incomplete Skewed and Circular Time Series, *Journal of Agricultural Biological and Environmental Statistics*, **17**, 544–567 (2012).
- [3] L. Landler, G.D. Ruxton, E.P. Malkemper, Advice on comparing two independent samples of circular data in biology, *Scientific Reports*, **11**, (2021).
- [4] B. Capaccioni, L. Valentini, M.B.L. Rocchi, G. Nappi, D. Sarocchi, Image analysis and circular statistics for shape-fabric analysis: applications to lithified ignimbrites, *Bulletin of Volcanology*, **58**, 501–514 (1997).
- [5] N.J.-S. Lee, K.W. Hoppel, S.A. Mango, A.R. Miller, Intensity and phase statistics of multilook polarimetric and interferometric SAR imagery, *IEEE Transactions on Geoscience and Remote Sensing*, **32**, 1017–1028 (1994).

- [6] J. Breckling, The analysis of directional time series: applications to wind speed and direction, *Springer Science & Business Media*, **61**, (2012).
- [7] C. Ley, T. Verdebout, *Modern Directional Statistics*, (2017).
- [8] J. Gill, D. Hangartner, Circular Data in Political Science and How to Handle It, *Political Analysis*, **18**, 316–336 (2010).
- [9] L.C. Astfalck, E.J. Cripps, J.P. Gosling, Hodkiewicz, I.A. Milne, Expert elicitation of directional metocean parameters, *Ocean Engineering*, **161**, 268–276 (2018).
- [10] P. Broly, J.-L. Deneubourg, Behavioural Contagion Explains Group Cohesion in a Social Crustacean, *PLoS Computational Biology*, **11**, e1004290 (2015).
- [11] A. García-González, A. Damon, F. Riverón-Giró, I. Ávila-Díaz, Circular distribution of three species of epiphytic orchids in shade coffee plantations, in Soconusco, Chiapas, Mexico, *Plant Ecology and Evolution*, **149**, 189–198 (2016).
- [12] R. Gatto, Saddlepoint Approximations to Tail Probabilities and Quantiles of Inhomogeneous Discounted Compound Poisson Processes with Periodic Intensity Functions, *Methodology and Computing in Applied Probability*, **14**, 1053–1074 (2011).
- [13] A. Marshall, A new method for adding a parameter to a family of distributions with application to the exponential and Weibull families, *Biometrika*, **84**, 641–652 (1997).
- [14] N. Eugene, C. Lee, F. Famoye, Beta-normal distribution and its applications, *Communication in Statistics- Theory and Methods*, **31**, 497–512 (2002).
- [15] K. Zografos, N. Balakrishnan, On families of beta- and generalized gamma-generated distributions and associated inference, *Statistical Methodology*, **6**, 344–362 (2008).
- [16] G.M. Cordeiro, M. De Castro, A new family of generalized distributions, *Journal of Statistical Computation and Simulation*, **81**, 883–898 (2010).
- [17] G.M. Cordeiro, E.M.M. Ortega, D.C.C. Da Cunha, The Exponentiated Generalized Class of Distributions, *Journal of Data Science*, **11**, 1–27 (2021).
- [18] G.M. Cordeiro, M. Alizadeh, P.R.D. Marinho, The type I half-logistic family of distributions, *Journal of Statistical Computation and Simulation*, **86**, 707–728 (2015).
- [19] F.V. Paula, A.D.C. Nascimento, G.J.A. Amaral, G.M. Cordeiro, Generalized Cardioid Distributions for Circular Data Analysis, *Stats*, **4**, 634–649 (2021).

- [20] S.R. Jammalamadaka, T. Kozubowski, A wrapped exponential circular model. *Proceedings of the AP Academy of Sciences*, **5**, 43-56 (2000).
- [21] A. Yilmaz, C. Biçer, A new wrapped exponential distribution, *Mathematical Sciences*, **12**, 285–293 (2018).
- [22] S.R. Jammalamadaka, A. SenGupta, *Topics in Circular Statistics*, (2001).
- [23] G.M. Cordeiro, A.J. Lemonte, E.M.M. Ortega, The Marshall–Olkin Family of Distributions: Mathematical Properties and New Models, *Journal of Statistical Theory and Practice*, **8**, 343–366 (2013).
- [24] P.H. Garthwaite, I.T. Jolliffe, I. Jolliffe, B. Jones, *Statistical inference*, Oxford University Press on Demand (2002).
- [25] J.J. Swain, S. Venkatraman, J.R. Wilson, Least-squares estimation of distribution functions in johnson’s translation system, *Journal of Statistical Computation and Simulation*, **29**, 271–297 (1988).
- [26] A. Pewsey, M. Neuhäuser, G.D. Ruxton, *Circular statistics in R*, Oxford University Press (2013).
- [27] C.P. Goodyear, Terrestrial and Aquatic Orientation in the Starhead Topminnow, *Fundulus notti*, *Science*, **168**, 603–605 (1970).
- [28] W.F. McDonough, Chemical and isotopic systematics of basalts and peridotite xenoliths: implications for the composition and evolution of the earth’s mantle, (1987).
- [29] M.A. Stephens, *Techniques for Directional Data*, (1969).
- [30] N.I. Fisher, T. Lewis, B.J.J. Embleton, *Statistical Analysis of Spherical Data*, (1987).